(2)

MARYLAND

COLLEGE PARK CAMPUS

Performance of the h-p Version of the Finite Element Method with Various Elements

by

I. Babuška

and

H. C. Elman

Technical Note BN-1128

September 1991

INSTITUTE FOR PHYSICAL SCIENCE AND TECHNOLOGY

Performance of the h-p version of the finite element method with various elements

I. Babuška[1]
H. C. Elman[2]

MD91-33-IBHE

TR91-33

September 1991

---

[1]Department of Mathematics and Institute for Physical Science and Technology, University of Maryland, College Park, MD 20742. The work of this author was partially supported by the U.S. Office of Naval Research under contract N00014-90-J-1030, and by the National Science Foundation under grant CCR-88-20279.

[2]Department of Computer Science and Institute for Advanced Computer Studies, University of Maryland, College Park, MD 20742. The work of this author was supported by the U.S. Army Research Office under grant DAAL-0389-K-0016, and by the National Science Foundation under grants ASC-8958554 and CCR-88-18340. Computer time was provided by the Advanced Computing Research Facility at Argonne National Laboratory.

Abstract. The paper addresses the performance of square elements of type Q(p) and Q'(p). (The Q(p) resp. Q'(p) are elements of degree p analogous to the well known 9 and 8 noded elements for p = 2.) The performance is analyzed theoretically for the class of analytic functions. Numerical experiments confirm the conclusions drawn from the theory. The computational complexity of a solution algorithm is studied using timings of the computation on an Alliant FX/8 computer. The data show that high order elements are preferable.

1. Introduction.

The difference between the performance of the 8 noded and 9 noded quadrilateral element has been directly and indirectly addressed in various contexts in the literature. The 8 noded element is sometimes called the serendipity element. In the mathematical literature [1] the 9 noded element is denoted as the Q(2) element while the 8 noded element is denoted as the Q'(2) element. Analogously, we can define elements Q(p) and Q'(p) for the general degree $p \geq 2$. As we will see in Section 2, the Q'(p) element is the element with minimal number of internal shape functions, while in Q(p) additional internal shapes are present. Of course, in general we can have less or more internal shape functions, in principle up to an infinite number of them. A natural question arises about optimal selection of the number of internal shape functions. This question is especially important in the context of the h-p version of the finite element method and its adaptive features.

The performance of the Q(p) and Q'(p) elements (and others, which differ by the number of the internal shape functions) can be compared from various points of view. In [2], [3] we addressed in detail the differences among various aspects of implementation on parallel computers. In [2], [4] we

addressed the question of the performance of iterative procedures. Here, in this paper we will be interested primarily in the question of the approximation properties (in the H^1-seminorm) of the $Q(p)$ and $Q'(p)$ elements and their computational effectivity for achieving prescribed accuracy.

The question of which element is preferable cannot be answered in general (see Section 8). This question can be addressed only in relation to a *class of functions* to be approximated. This class has to be adequate to the problems solved in practice. In this paper we consider the *class of analytic functions*. This class is very natural for static structural mechanics problems where the solutions satisfy an elliptic differential equation with piecewise analytic right hand side and boundary conditions on a domain Ω with piecewise analytic boundary. The performance of the $Q(p)$ and $Q'(p)$ elements will be related to distance of the element to the boundary of the analyticity domain of the approximated function.

Obviously the $Q'(p)$ element has a smaller number of the shape functions. Hence, we can ask what is the smallest number $\mathcal{H} > 1$ such that the $Q'(\mathcal{H}p)$ element yields a better approximation than the $Q(p)$ element for a particular approximated function (or class of functions). The number $\mathcal{H}$ can be used as a natural comparison index. We can use this index together with some other complexity indicator to assess the computational performance. For example in [2], [3] we have used the value $\mathcal{H} = \sqrt{2}$ when we analyzed the complexity of parallel computations.

In this paper we will present a theoretical upper estimate for the index $\mathcal{H}$ when the approximation is measured in the H^1-seminorm. Further, we will present the results of various numerical experiments on a model example. In additions, some comparisons between quadrilateral and triangular elements will be given, as well the relation between the mesh sizes and the degree of ele-

ments leading to the minimal computational cost for a given requested accuracy.

2. The Q(p) and Q'(p) elements.

Denote by $S = \{|x| < 1/2, \ |y| < 1/2\}$ the unit square and by Γ_i, $i = 1,2,3,4$ its sides, as indicated in Figure 2.1; let $\Gamma = \bigcup_{i=1}^{4} \Gamma_i = \partial\Omega$

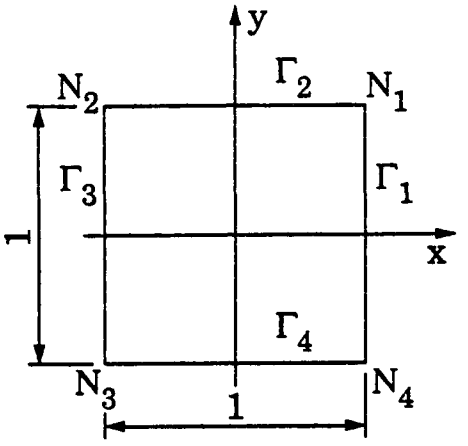

Figure 2.1. Scheme of the square domain.

In contrast to [1], we define the spaces Q(p) and Q'(p) via listing the *nodal*, *side* and *internal* shape functions as introduced in [5].

α) The Q(p) elements. Here we define

a) *the nodal shape functions associated with the nodes* N_i:

$$
\begin{aligned}
N_1 : &\quad \phi_1(x,y) = (1/2 + x)(1/2 + y), \\
N_2 : &\quad \phi_2(x,y) = (1/2 - x)(1/2 + y), \\
N_3 : &\quad \phi_3(x,y) = (1/2 + x)(1/2 - y), \\
N_4 : &\quad \phi_4(x,y) = (1/2 - x)(1/2 - y).
\end{aligned}
\tag{2.1}
$$

b) *the side shape functions associated with the sides* Γ_i:

$$
\begin{aligned}
&\Gamma_1: \quad \psi_{1,j}(x,y) = P_j(y)(1/2 + x), \quad j = 2,3,\ldots,p,\\
&\Gamma_2: \quad \psi_{2,j}(x,y) = P_j(x)(1/2 + y), \quad j = 2,3,\ldots,p,\\
&\Gamma_3: \quad \psi_{3,j}(x,y) = P_j(y)(1/2 - x), \quad j = 2,3,\ldots,p,\\
&\Gamma_4: \quad \psi_{4,j}(x,y) = P_j(x)(1/2 - y), \quad j = 2,3,\ldots,p.
\end{aligned}
\tag{2.2}
$$

Here $P_j(x)$ is a polynomial of degree j such that $P_y(\pm 1/2) = 0$. Specifically we use, $P_j(x) = \sqrt{\frac{2j-1}{2}} \int_{-1}^{2x} L_{j-1}(t)dt$, $j = 2,3,\ldots,p$ where $L_j(t)$ is the Legendre polynomial of degree j. For more see e.g., [5].

c) *The internal shape functions for the* Q(p) *element*:

$$\rho_{i,j}(x,y) = P_i(x)\,P_j(y) \qquad i,j = 2,\ldots,p. \tag{2.3}$$

The space of the Q(p) elements is the span of its nodal, side and internal shape functions.

β) <u>The Q'(p) elements</u>. Here the *nodal* and *side* shape functions *are the same* as in the family Q(p) i.e., they are given by (2.1) and (2.2).

c') *The internal shape functions for the* Q'(p) *element*:

$$\rho_{i,j}(x,y) = P_i(x)\,P_j(y), \qquad i,j, \geq 2, \quad i+j \leq p.$$

The space of the Q'(p) elements is the span of its nodal, side and shape functions.

The Q(p) and Q'(p) elements can be described by listing all of the *monomials* belonging to their space. We can visualize them in the Pascal table of Figure 2.2.

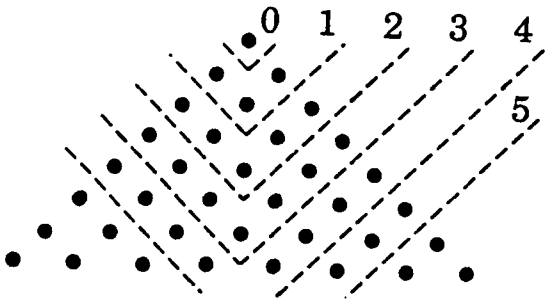

Figure 2.2. The Pascal table for the Q(p) element.

Every bullet in the Pascal table depicts the term $x^j y^{p-j}$. The Q(p) element is then associated with the set of the bullets in the diamond area shown in Figure 2.2. The value of p is shown there too. Analogously we depict the Pascal table for the Q'(p) element (see Figure 2.3).

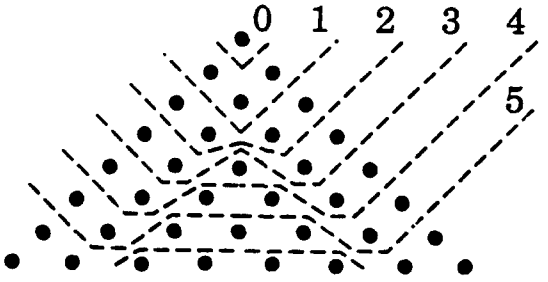

Figure 2.3. The Pascal table for the Q'(p) element.

The Q'(p) space is the smallest space of polynomials including the polynomials of *total* degree p and the side functions which are polynomials of degree p on one side and zero on the three others.

It is easy to compute the dimension of the spaces $Q(p)$ and $Q'(p)$. We have

$$\text{Dimension of } Q(p) = (p+1)^2$$

$$\text{Dimension of } Q'(p) = \begin{cases} 4 & \text{for } p = 1 \\ 8 & \text{for } p = 2 \\ 4p + \dfrac{(p-2)(p-3)}{2} & \text{for } p \geq 3 \end{cases}$$

In the next section we will also employ the space $Q(p,q) = Q'(p,q)$, with

$$Q(p,q) = Q''(p) \oplus Z(q)$$

$$Z(q) = \text{span}\{P_i(x)\, P_j(y), \quad 0 \leq i,j \leq q\}$$

and

$$Q'(p,q) = Q''(p) \oplus Z'(q)$$

$$Z'(q) = \text{span}\{P_i(x)\, P_j(y), \quad 0 \leq i+j \leq q\}$$

where $Q''(p)$ is the span of the nodal and side functions only. We have $Q(p,p) = Q(p)$ and $Q'(p,p) = Q'(p)$. The spaces $Z(q)$ and $Z'(q)$ consist only of internal shape functions.

We also introduce

$$Q(p,\infty) = Q''(p) \oplus H_0^1(S) = Q'(p,\infty)$$

where $H_0^1(S)$ is the standard Sobolev space with zero traces on Γ.

3. The model problem.

Let $x + iy = z \in \mathbf{C}$, $z_0 = \frac{1}{2}(1+i)$, $a > 1$ and

$$(3.1) \qquad w_o^{(a)}(z) = \frac{1}{a^2-(z+z_0)^2} + \frac{1}{a^2+(z+z_0)^2} - \left(\frac{1}{a^2-1} + \frac{1}{a^2+1}\right).$$

The function $w_0^{(a)}(z)$ is a holomorphic function of the complex variable z

on $S = \{|x| < 1/2,\ |y| < 1/2\}$. Denote

$$u_0^{(a)} = \mathrm{Re}\, w_0^{(a)}, \qquad v_0^{(a)} = \mathrm{Im}\, w_0^{(a)}; \tag{3.2}$$

then $u_0^{(a)}$ and $v_0^{(a)}$ are harmonic on S.

Let $H^1(S)$ be the real (or complex) Sobolev space. For $u,v \in H^1(S)$ let

$$[u,v] = \int_S (\nabla u \cdot \overline{\nabla v})\, dxdy \tag{3.3}$$

$$|u|^2 = \int_S |\nabla u|^2\, dxdy \tag{3.4}$$

be the scalar product and seminorm in $H^1(S)$. From the Cauchy-Riemann condition we have

$$|u_0^{(a)}| = |v_0^{(a)}|$$

and

$$|w_0^{(a)}|^2 = |u_0^{(a)}|^2 + |v_0^{(a)}|^2. \tag{3.5}$$

Let us consider the Neumann problem for the Laplace equation on S

$$-\Delta u = 0 \qquad \text{on } S \tag{3.6}$$

$$\frac{\partial u}{\partial n} = g \qquad \text{on } \Gamma \tag{3.7}$$

where g is such that the solution of (3.6) and (3.7) is $u_0^{(a)}$. Because the solution u of (3.6) and (3.7) is determined up to a constant, we will assume that $u(-1/2, 1/2) = u_0^{(a)}(-1/2, 1/2)$. Note that we are interested in the seminorm $|\cdot|$, and hence this constant is not essential.

For any $a > 1$, $D^\alpha u_0^{(a)} = \dfrac{\partial^{|\alpha|} u_0^{(a)}}{\partial x^{\alpha_1} \partial y^{\alpha_2}} \in H^1(S)$ for any multindex $\alpha = (\alpha_1, \alpha_2)$ $\alpha_1 \geq 0$, $\alpha_2 \geq 0$, integers, $|\alpha| = \alpha_1 + \alpha_2$. Nevertheless as $a \to 1$, $|D^\alpha u^{(a)}| \to \infty$ and hence $u_0^{(a)}$ becomes less smooth as a decreases. The function $u_0^{(a)}$ is analytic on $\bar{S}$ and its analyticity domain is $\Omega =$

$R^2 \setminus \{z = \pm a - z_0, \quad \pm ia - z_0\}$. This function is a typical representative of the solutions of elliptic PDE problems in two dimensions. In practice such solutions are analytic with singularities only at a finite number of points on the boundary of the domain, e.g., where the boundary has corner or the boundary condition type is changing.

We will be interested in the performance of the finite element method for solving (3.6) and (3.7) where the exact solution is $u_0^{(a)}$ and the mesh consists of squares with sides of length $\frac{1}{\ell}$ (i.e., S is divided into ℓ^2 squares).

Let

$$\hat{Q}'(p) = \{u \in Q'(p) | \quad u \text{ is harmonic polynomial}\}.$$

Obviously we have

$$Q(p,\infty) \supset Q(p) \tag{3.9}$$

$$Q'(p) \supset \hat{Q}'(p). \tag{3.10}$$

We denote by $u_0^{(a)}(Q(p),\ell)$, $u_0^{(a)}(Q'(p),\ell)$, $u_0^{(a)}(Q(p,\infty),\ell)$, $u_0^{(a)}(\hat{Q}'(p),\ell)$ the finite element solution of (3.6) (3.7) using the respective $Q(p)$ and $Q'(p)$ element etc. on the mesh consisting by ℓ^2 squares. The finite element solution is the projection of $u_0^{(a)}$ on the set of finite element functions. We will impose the constraint at (-1/2, 1/2) that the finite element solution coincides with the exact solution $u_0^{(a)}$ to get uniqueness. This constraint does not influence the seminorm $|\cdot|$.

Denote

$$\eta^{(a)}(Q(p),\ell) = \frac{|u_0^{(a)} - u_0^{(a)}(Q(p),\ell)|}{|u_0^{(a)}|}$$

and analogously $\eta^{(a)}(Q'(p),\ell)$ $\eta^{(a)}(Q(p,\infty),\ell)$, $\eta^{(a)}(\hat{Q}(p),\ell)$. For any $a >$

1 we have

$$\eta^{(a)}(Q(p,\infty),\ell) \le \eta^{(a)}(Q(p),\ell) \le \eta^{(a)}(Q'(p),\ell) \le \eta^{(a)}(\hat{Q}'(p),\ell)$$

and

$$\eta^{(a)}(Q'(2p),\ell) \le \eta^{(a)}(Q(p)\ell)$$

Let

$$(3.11) \qquad \mathcal{H}^{(a)}(p,\ell) = \inf\{\sigma,\ \sigma > 1 \mid \eta^{(a)}(Q'(\sigma p),\ell) \le \eta^{(a)}(Q(p),\ell)\}$$

The index $\mathcal{H}^{(a)}(p,\ell)$ is a good characterization of the performance of the $Q(p)$ and $Q'(p)$ elements relative to the function $u_0^{(a)}$ (and mesh composed by ℓ^2 elements)

Let us further define

$$(3.12) \qquad \mathcal{T}^{(a)}(p,\ell) = \inf\{\sigma,\ \sigma>1 \mid \eta^{(a)}(\hat{Q}'(\sigma p),\ell) \le \eta^{(a)}(Q(p,\infty),\ell)\}$$

Obviously $\mathcal{T}^{(a)}(p,\ell) \ge \mathcal{H}^{(a)}(p,\ell)$ and hence $\mathcal{T}^{(a)}(p,\ell)$ is an upper bound for $\mathcal{H}^{(a)}(p,\ell)$.

If $\ell = 1$ we often will not write the index ℓ. For example, we will write $\eta^{(a)}(Q(p))$ instead $\eta^{(a)}(Q(p),1)$, $\mathcal{T}^{(a)}(p)$ instead $\mathcal{T}^{(a)}(p,1)$, etc.

4. Asymptotic estimate of $\mathcal{T}^{(a)}(p)$, $\ell = 1$.

Let

$$(4.1) \qquad \mu_i^{(a)}(p) = \inf_{\omega\in P_i(p)} |u_0^{(a)} - \omega|_{H^{1/2}(\Gamma_i)} / |u_0^{(a)}| \qquad i = 1,\ldots,4$$

Here $P_i(p)$ is the set of all polynomials on Γ_i, $i = 1,2,3,4$, of degree p. By $|\cdot|_{H^{1/2}(\Gamma_i)} = \inf_{\psi\in A_i(\varphi)} |\psi|$, $A_i(\varphi) = \{\psi \mid \psi$ is harmonic on S and $\psi = \varphi$ on $\Gamma_i\}$ we denote the standard $H^{1/2}(\Gamma_i)$ seminorm of the traces on

Γ_i. Then by the extension theorem we have

$$\eta^{(a)}(Q(p,\infty)) \geq \max_{1\leq i\leq 4}\left(\mu_i^{(a)}(p)\right) = \mu^{(a)}(p). \tag{4.2}$$

Further we have

$$|u_0^{(a)}|\eta^{(a)}(\hat{Q}'(p)) \leq \inf_{w\in\hat{Q}^c(p)} |w_0^{(a)} - w| \tag{4.3}$$

where $\hat{Q}^c(p)$ is the space of all complex polynomials of degree $\leq p$.

Now we apply the classical theory of approximation of functions in complex domain [6]. First we will consider the approximation on Γ_i. To this end let

$$I = \{z = x + iy,\ |x| \leq 1/2,\ \ y = 0\} \subset \mathbb{C}$$

and

$$\Omega^I = \{z \in \mathbb{C},\ \ z \notin I\}$$

The function

$$\phi(\zeta) = \frac{1}{4}(\zeta + \frac{1}{\zeta}), \qquad \zeta = \xi + i\eta \tag{4.4}$$

maps the $\gamma = \{\zeta \mid |\zeta| > 1\}$, i.e., the outside of the unit circle in the ζ-plane) onto Ω^I.

Let $\varphi(z)$ be a holomorphic function in a domain $\mathcal{D} \subset \mathbb{C}$, $I \subset \mathcal{D}$ and $\varphi(z)$ is real for $z \in I$. Define $\Phi(\zeta) = \varphi(\phi(\zeta))$. Then $\Phi(\zeta)$ is a holomorphic function in an annulus

$$\sum_R = \{\zeta \mid 1 < |\zeta| < R\}$$

for certain R which depends on the domain of analyticity $\mathcal{D}$ of the function φ. We assume that $\sum_R$ is the largest possible annulus, i.e., $\Phi(\zeta)$ is not holomorphic in the annulus $\sum_{R+\varepsilon}$ for any $\varepsilon > 0$.

From [6] §5.2, Theorem 3, we have for any $\varepsilon > 0$ and $k = 0,1$

$$(4.5)\qquad C_1(\varepsilon)(R+\varepsilon)^{-p} \le \inf_{\omega\in\mathcal{P}^c(p)} \left(\int_I |\varphi^{(k)}-\omega|^2 dx\right)^{1/2} \le C_2(\varepsilon)(R-\varepsilon)^{-p}$$

where $\mathcal{P}^c(p)$ is the set of all complex polynomials on I of degree $\le p$ and $C_1(\varepsilon)$, $C_2(\varepsilon)$ are constants independent of p.

Using the standard interpolation theory in Banach spaces [7] we get from (4.5)

$$(4.6)\qquad C_1(\varepsilon)(R+\varepsilon)^{-p} \le \inf_{\omega\in\mathcal{P}^c(p)} |\varphi-\omega|_{H^{1/2}(I)} \le C_2(\varepsilon)(R-\varepsilon)^{-p}$$

Here $|\psi(x,y)|_{H^{1/2}(I)} = |\psi(x, y+1/2)|_{H^{1/2}(\Gamma_2)}$. We note that if $\varphi(x)$ is real on I then we can replace in (4.5) the space $\mathcal{P}^c(p)$ of complex polynomials by the space $\mathcal{P}(p)$ of real polynomials.

For $i = 1$ let

$$w_1(z) = w_1(x+iy) = \frac{1}{2}\left[w(x+iy) + \overline{w(1-x+iy)}\right],$$

then $w_1(z)$ is a holomorphic function in a domain $\mathcal{D}_1 \subset \mathbb{C}$, $\Gamma_1 \subset \mathcal{D}$ and $w_1(z) = u_0(z)$ for $z \in \Gamma_1$. Analogously we define $w_i(z)$, $i = 2,3,4$. We use now (4.6) for the functions $w_i(z)$ instead of $\varphi(z)$.

Relation (4.6) now leads in our particular case immediately to the estimate

$$(4.7)\qquad C_1(\varepsilon)(R^{(1)}+\varepsilon)^{-p} \le \mu^{(a)}(p) \le C_2(\varepsilon)(R^{(1)}-\varepsilon)^{-p}$$

where

$$(4.8)\qquad R^{(1)} = \min\left[|\zeta_1|, |\zeta_2|\right]$$

with

$$\phi(\zeta_1) = (a-1) + 1/2$$

$$\phi(\zeta_2) = \frac{1}{2} + i(a-1)$$

Then we get from (4.2) and (4.7)

$$(4.9)\qquad \mu^{(a)}(p) \ge C(\varepsilon)(R^{(1)}+\varepsilon)^{-p}$$

Because for large ζ we have

$$\phi(\zeta) \approx \frac{1}{4}\zeta \tag{4.10}$$

we get for large a

$$\eta^{(a)}(Q(p,\infty)) \geq C_1(\varepsilon)(4a+\varepsilon)^{-p} \tag{4.11}$$

We will now consider the estimate for $\eta^{(a)}(\hat{Q}'(p))$. By the same argument as above let $\psi(\zeta)$ denote the conformal mapping of the outside of the unit circle γ onto the outside of S. Using the Schwarz Christoffel formula (see [8],[9]) we get with $\hat{z}_0 = \sqrt{2}\, z_0$, $|\hat{z}_0| = 1$

$$\frac{dz}{d\zeta} = \psi'(\zeta) = c\,\frac{(\zeta^2 - \hat{z}_0^2)^{1/2}(\zeta^2 + \hat{z}_0^2)^{1/2}}{\zeta^2} \tag{4.12}$$

with $c = 0.591$ obtained by numerical integration. The function $\psi(\zeta)$ now plays the same role as the function $\phi(\zeta)$ in (4.4).

Let

$$R^{(2)} = \min_{1\leq i\leq 4} |\zeta^{(i)}| \tag{4.13}$$

where

$$\psi(\zeta^{(1)}) = a + z_0$$

$$\psi(\zeta^{(2)}) = -a + z_0$$

$$\psi(\zeta^{(3)}) = ia + z_0$$

$$\psi(\zeta^{(4)}) = -ia + z_0$$

Then we get analogously as before

$$\eta^{(a)}(\hat{Q}'(p)) \leq C_2(\varepsilon)(R^{(2)}-\varepsilon)^{-p}. \tag{4.14}$$

Because for large ζ we have

$$\psi(\zeta) \approx 0.591\,\zeta$$

we get for large a

$$\eta^{(a)}(\hat{Q}'(p)) \le C_2(\varepsilon)(0.591^{-1}a - \varepsilon)^{-1} = C_2(\varepsilon)(1.692a - \varepsilon)^{-p} \tag{4.15}$$

Remark 4.1. From the Lindelöf principle, we always have $R^{(1)} > R^{(2)}$.

From (4.11), (4.15), and (3.12) we see that for *large* a,

$$\mathcal{F}^{(a)}(p) \le \beta \tag{4.16}$$

where

$$\frac{(1.692a)^{\beta p}}{(4a)^p} > \frac{C_1(\varepsilon)}{C_2(\varepsilon)} \tag{4.17}$$

and hence for large a and p we get $\beta \approx 1$ and hence also $\mathcal{H}^{(a)} \approx 1$.

On the other hand it is easy to see that for small a, $R^{(1)} - 1 = O((a-1)^{1/2})$ and $R^{(2)} - 1 = O((a-1)^{2/3})$. Hence for small a $\beta \longrightarrow \infty$ and we can expect that with decreasing a, $\mathcal{H}$ will grow. Of course always $\mathcal{H} \le 2$.

5. Numerical examples. Performance of the Q(p) and Q'(p) elements in the p-version - $\ell = 1$.

In Figure 5.1 we show the graphs of $\eta^{(a)}(Q(p))$ and $\eta^{(a)}(Q'(p))$ as functions of a and p in the scale $\lg \eta^{(a)} \times p$. This scale is associated with the expected behavior $\eta^{(a)} \approx (R(a))^{-p}$ in which case we would get a straight line. In Table 5.1 we give the values of $R^{(i)}$, i = 1,2, with $\eta^{(a)}(Q(p,\infty))$ $(R^{(1)})^{-p}$ from (4.8) and with $\eta^{(a)}(\hat{Q}'(p)) \approx (R^{(2)})^{-p}$ from (4.13).

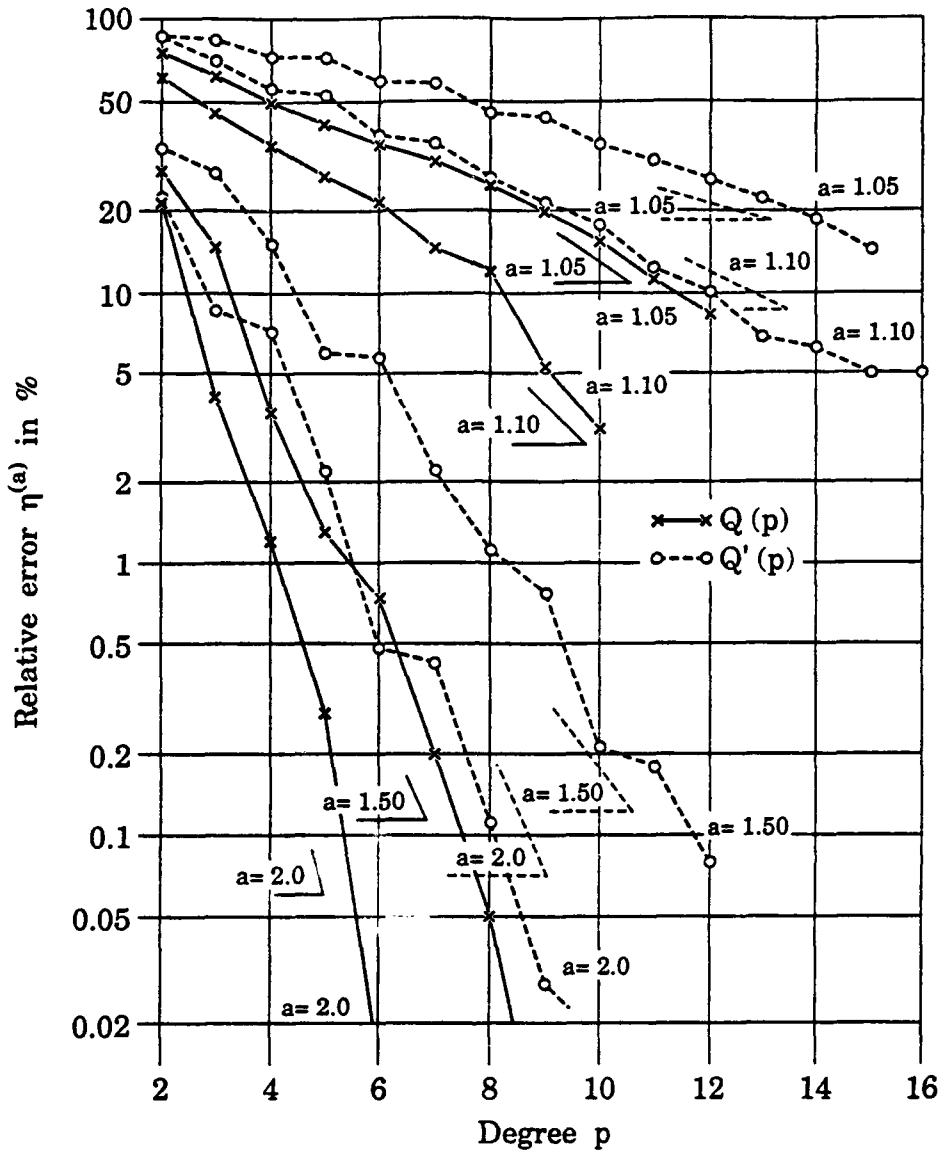

Figure 5.1. Performance of the Q(p) and Q'(p) elements for various a.

Table 5.1. The rates $R^{(i)}$, i = 1,2

a	$R^{(1)}$	$R^{(2)}$
1.05	1.39	1.13
1.10	1.60	1.25
1.50	2.81	1.86
2.00	3.97	2.38

In Figure 5.1 we also show theoretical slopes for $\eta^{(a)}(Q(p,\infty))$ and $\eta^{(a)}(\hat{Q}'(p))$ which are expected approximations of the rates of $\eta^{(a)}(Q(p))$ and $\eta^{(a)}(Q'(p))$ respectively. We see that in fact the theoretical slope of $\eta^{(a)}(Q(p,\infty))$ is close to the one of $\eta^{(a)}(Q(p))$ (but is slightly larger) and the slope of $\eta^{(a)}(Q'(p))$ is slightly larger than that of $\eta^{(a)}(\hat{Q}'(p))$ as should be expected.

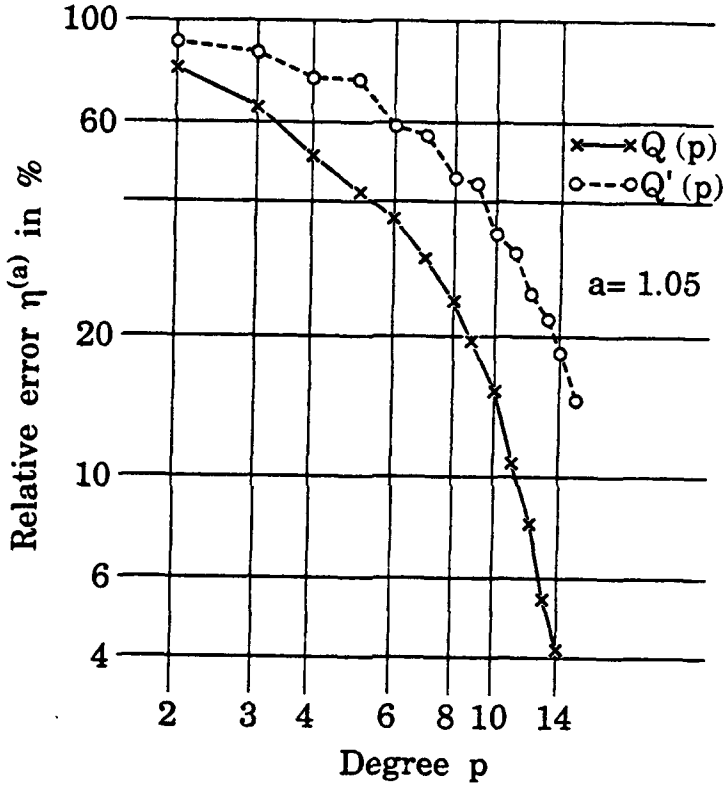

Figure 5.2a. Comparison of the performance of the Q(p) and Q'(p) elements for a = 1.05.

Figure 5.2a shows the error $\eta^{(a)}(Q(p))$ and $\eta^{(a)}(Q'(p))$ on a $\lg \eta \times \lg p$ scale for a = 1.05. We see that the curves are nearly parallel and

$$\eta^{(a)}(Q'(p\sigma(p))) = \eta^{(a)}(Q(p))$$

where for small p, $\sigma(p) \approx 1.8$ and for larger p, $\sigma(p) \approx 1.4$. Figure 5.2b shows the analogous graphs for a = 2.0. Here we see $1.3 < \sigma(p) < 1.6$. This

indicates, as the analyses support, that σ decreases as a increases, i.e., as the smoothness of the solution increases.

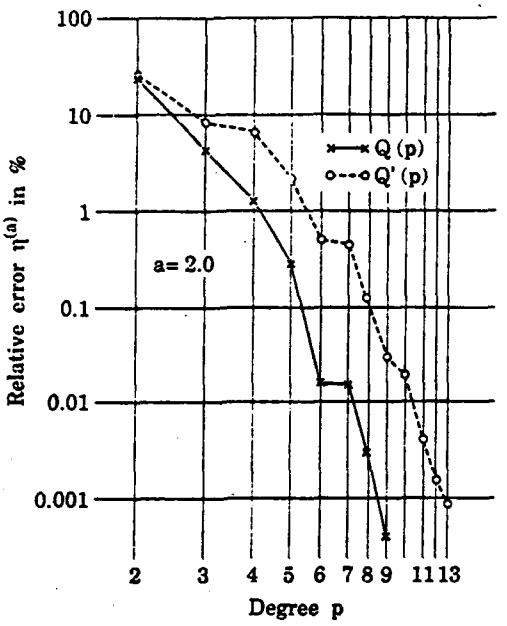

Figure 5.2b. Comparison of the performance of the Q(p) and Q'(p) elements for a = 2.

We have seen that the difference among the spaces Q(p). Q'(p), Q(p,q), Q'(p,q) differ only in the different number of internal shape functions. In Figure 5.3a,b we show the error $\eta^{(a)}(Q(p,q))$ and $\eta^{(a)}(Q'(p,q))$ for q

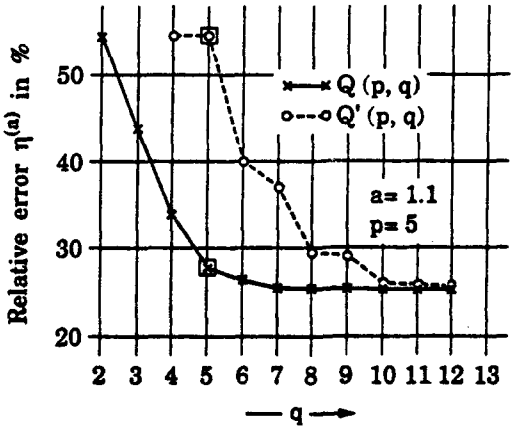

Figure 5.3a. Influence of the internal shape functions on the accuracy for a = 1.1 and p = 5, for the Q(p) and Q'(p) elements.

increasing, $p = 5,7$ and $a = 1.1$. The value $p = q$ is marked in the figure. This value is almost optimal for the Q element but is far from the optimal for the Q' element. As $a \to \infty$ the influence of the internal shape functions decreases.

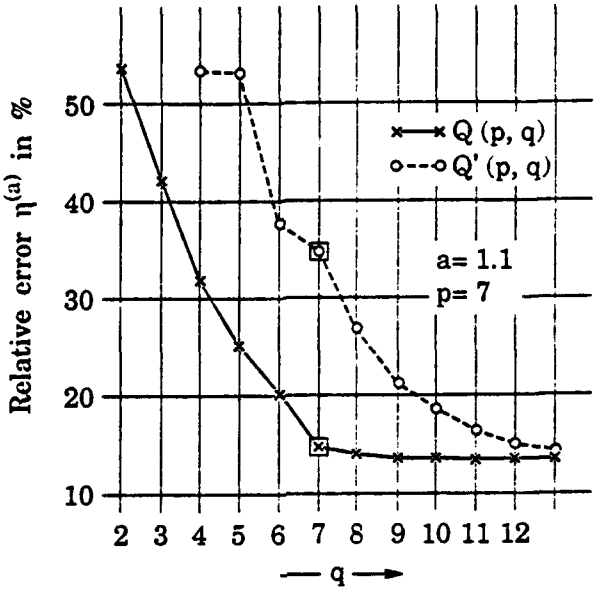

Figure 5.3b. Influence of the internal shape functions on the accuracy for $a = 1.1$ and $p = 7$ for the Q(p) and Q'(p) elements.

6. Performance of the Q(p) and Q'(p) elements in the h-p version - $\ell > 1$.

In Section 5 we analyzed the case when $\ell = 1$, i.e., the domain S on which the problem (3.6)-(3.7) has been solved was not partitioned. Let us assume now that $\ell > 1$, i.e., S is divided into ℓ^2 squares. We can now expect that the error can be essentially estimated element by element. It has been seen that the approximation was governed in the case $\ell = 1$ by the parameter a with a-1 being the ratio of the distance of the singularity to the boundary and size of the element. (Note that S is unit square.) Denote by $\eta^{(a)}(\ell)$ the error when ℓ^2 elements are used. Then for ℓ not too large,

the error is governed by the "worst" element, i.e., the one closest to the singularity. Then we can approximately expect

$$\eta^{(a)}(\ell) \approx \eta^{((a-1)\ell+1)}(1) \tag{6.1}$$

where by $\eta^{(a)}(\ell)$ we denote the relative error when ℓ^2 elements are used.

In Figure 6.1a,b we show the error $\eta^{(a)}(Q(p),\ell)$ and $\eta^{(a)}(Q'(p),\ell)$ for $a = 1.05$. In addition, we show in the figure the error $\eta^{(\tilde{a})}(Q(p),\ell)$ for $\tilde{a} \approx (a-1)\ell + 1$. We see that (6.1) nearly holds. For other values of a the results are similar.

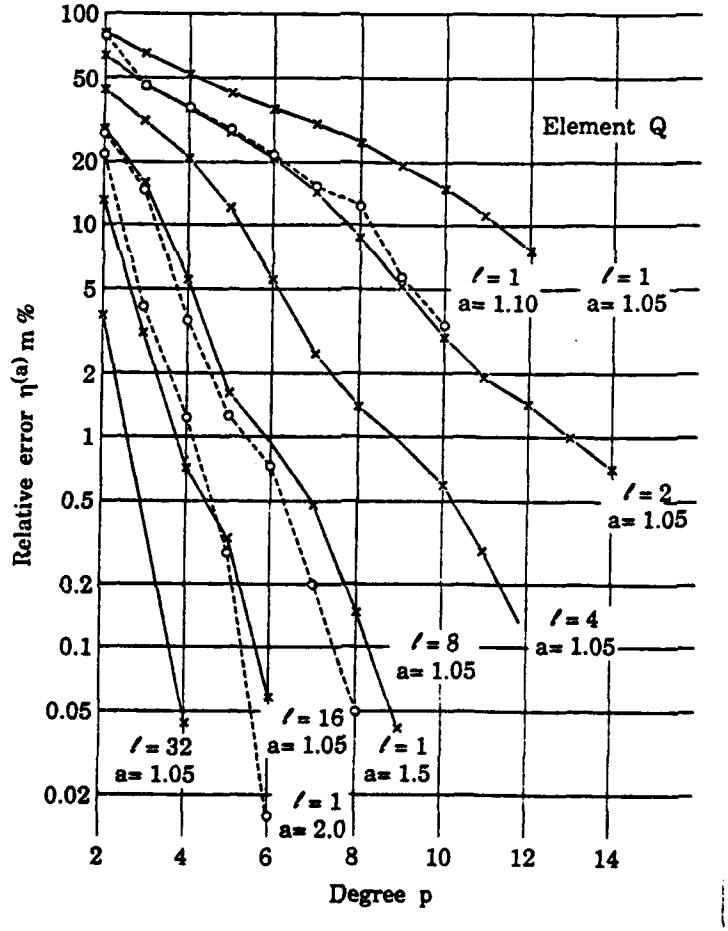

Figure 6.1a. Comparison of the performance of the Q(p) element for different a and ℓ leading approximately to the same accuracy.

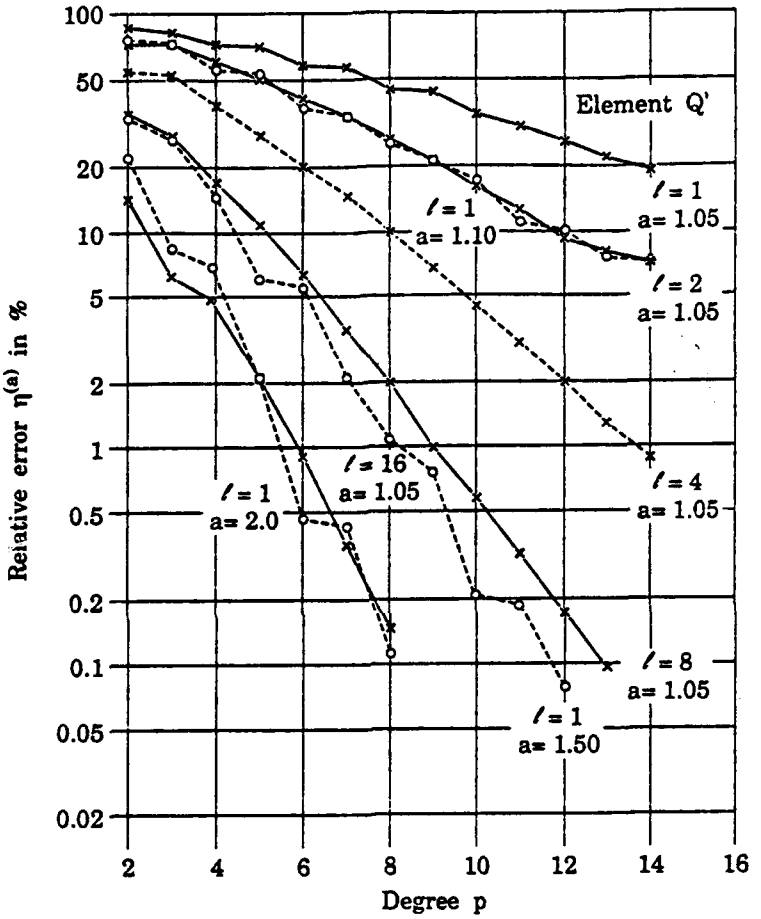

Figure 6.1b. Comparison of the performance of the Q'(p) element for different a and ℓ leading to approximately the same accuracy.

In Figure 6.2 we show $\eta^{(a)}(Q(p,q),\ell)$ for a = 1.1, p = 5 and various q and ℓ. The values $\eta^{(a)}(Q(p),\ell) = \eta^{(a)}(Q(p,p),\ell)$ are marked. We see that for $\ell > 1$ the character does not change.

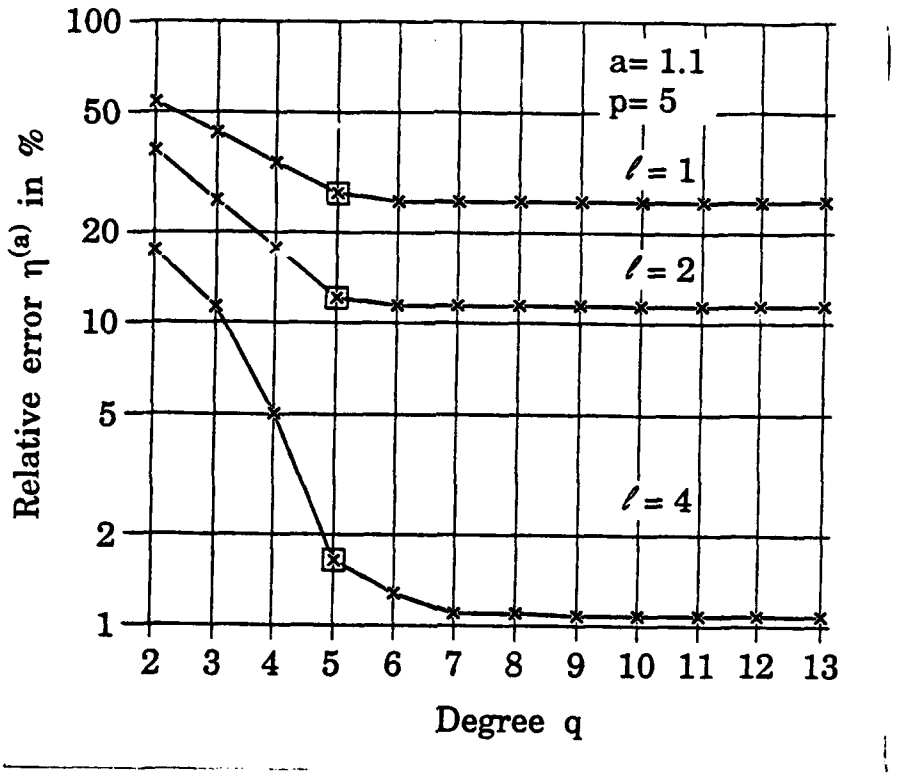

Figure 6.2. Performance of the Q(p,q) element for a = 1.1 and p = 5.

7. Comparison of the performance of the triangular elements and Q(p) elements.

So far we have discussed square elements. Analogously, the triangular elements of degree p can be constructed (see [5]). Here the space T(p) of the triangular element consists of all polynomials of degree $\leq$ p.

Let us consider once more a square element. Dividing it into two triangles by the diagonal and using T(p) elements we can understand this as a *composite element* which has the same degrees of freedom as the element Q(p).

We can also enrich the space T(p) by internal functions as in the case of square elements. The analysis of the kind we have made in Section 4 can here be used, too.

Based on this analysis we can expect that the performance of the Q(p) element is better than of T(p) and the performance of Q(p) improves with increasing p and the smoothness of the approximated function. These conclusions are in agreement with numerical tests. In Figure 7.1 we show $\eta^{(a)}(T(p),\ell)$ and $\eta^{(a)}(Q(p),\ell)$ for $a = 1.05$ and various p and ℓ.

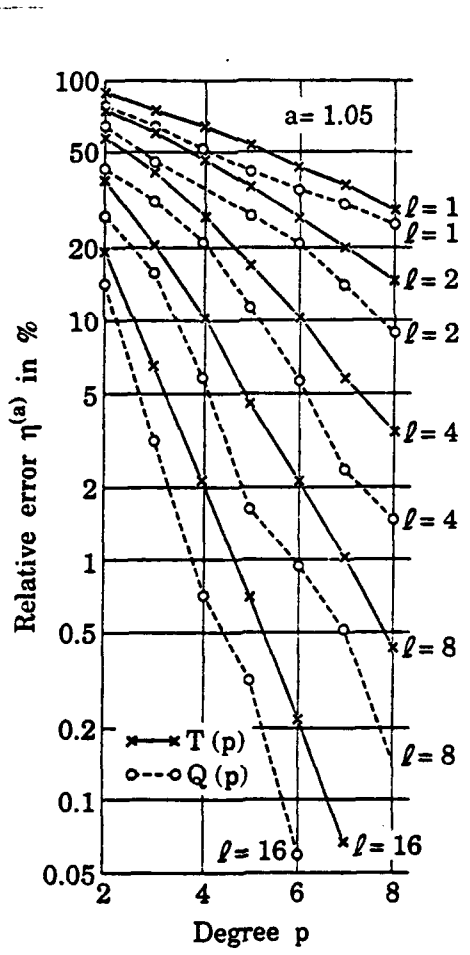

Figure 7.1. Comparison of the performance of the square and triangular element.

8. Additional considerations.

It is obvious that in general it is impossible to prefer either element $Q(p)$ or $Q'(p)$. The preference depends strongly on the class of solutions under consideration. To illustrate this let us be interested for simplicity in the best approximations of u on S in the L_2-norm instead of the $H^1(S)$ seminorm, i.e., let us consider

$$\inf \int_S (u_0-w)^2 \, dxdy$$

where the infimum is taken over all functions of $Q(p)$ resp. $Q'(p)$. In this case we will consider shape functions of the form $L_i(x)\cdot L_j(y)$ where $L_j(x)$ is the normalized Legendre polynomial of degree j. Then we can write

$$u_0 = \sum_{i,j=1}^{\infty} c_{ij} L_i(x) L_j(x) \tag{8.1}$$

and

$$\inf_{w \in Q(p)} \int_S (u_0-w)^2 \, dxdy = \sum_{i,j>p} c_{ij}^2 \tag{8.2}$$

$$\inf_{w \in Q'(p)} \int_S (u_0-w)^2 \, dxdy = \sum_{i+j>p} c_{ij}^2 \tag{8.3}$$

In Figure 8.1 we depict the pairs (i,j) in the upper quarter plane by bullets; then the error of $Q(p)$ resp. $Q'(p)$ is the sum of the squares of all coefficients c_{ij} associated with the bullets outside the square resp. triangle shown in Figure 8.1. Hence the performance of the element depends on the distribution of c_{ij} for the approximated functions resp. class of functions under consideration. If for small (i,j) the coefficients are decaying slowly and are approximately of the same magnitude then the

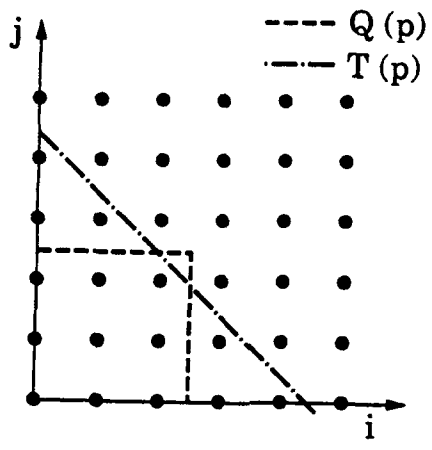

Figure 8.1. Schematic comparison of the Q(p) and Q'(p) element.

coefficient $\mathcal{H}$ introduced in (3.11) will have approximately the value $\sqrt{2}$. We have roughly seen this in our numerical experiments with a = 1.05.

We remark that it is easy to introduce a class of functions for which either Q(p) or Q'(p) elements are preferable for this class.

Although we addressed for simplicity the L_2-norm, the same conclusions are the same for the H^1-seminorm.

9. Optimal relation between p and ℓ.

The optimal relation between p and ℓ can be based on various criteria. In Figure 9.1 we show the relation between the number of degrees of freedom for which $\eta^{(a)}(Q(p),\ell) = \varepsilon$, a = 1.05, for various p and ε. With this criterion, we see that use of higher p is preferable.

In general, of course, cost is not proportional to the number of degrees N. We can also determine optimality in terms of the computational complexity (cost) needed to solve the problem (3.6) (3.7) with an accuracy ε. To address this question, we examine the CPU times required to achieve a specified accuracy for the implementation of a finite element solver described

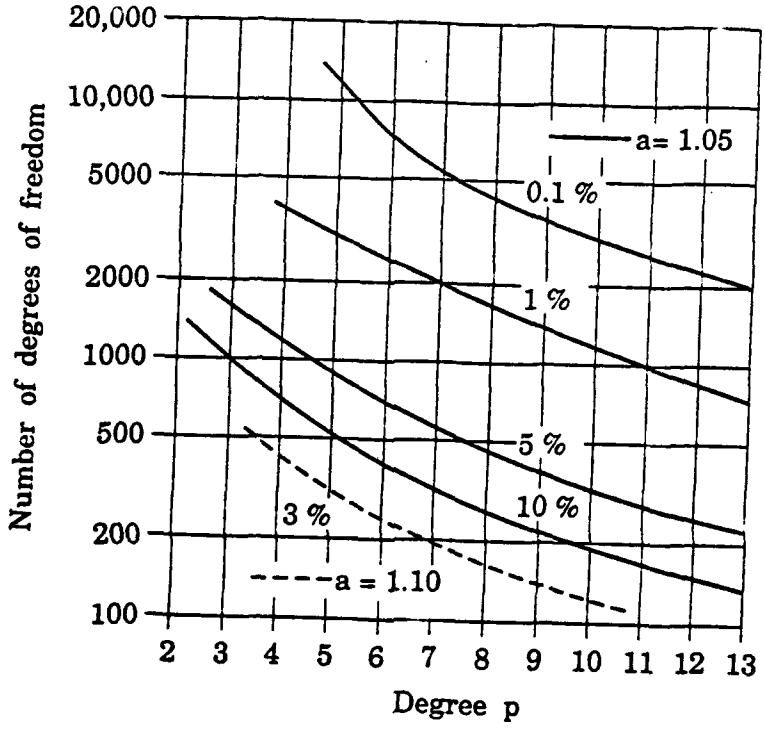

Figure 9.1. Number of degrees of freedom leading to the same accuracy for the element $Q(p,\ell)$.

in [3]. The algorithm used treats the unknowns associated with internal shape functions in a manner akin to domain decomposition, in which these unknowns are decoupled from the system using static condensation. The resulting global interface problem is then solved iteratively using a preconditioned conjugate gradient algorithm, with the preconditioner derived from the portion of the global stiffness matrix associated with the nodal points, i.e., $p = 1$. See [4] for an analysis of this preconditioner. The implementation was made on an eight processor Alliant FX/8 parallel computer, with options to run on fewer

than eight processors also available. Further details about the algorithm and its implementation, as well as a detailed study of performance characteristics, can be found in [3].

Our concern is the cost, in CPU time, required to achieve a specified accuracy. The computations reported here correspond to choosing values of ℓ and p that produce a given accuracy and then solving the model problem (3.6)-(3.7) with zero right hand side. In all cases, the conjugate gradient iteration started with a random initial guess with entries between 0 and 1, and the stopping criterion was that the relative error in the energy norm be less than 0.5×10^{-3}. (This is smaller than accuracy considered.) All computations were performed using double precision FORTRAN.

Table 9.1 shows the CPU time in seconds on *one* processor for various ℓ that produces solution with accuracy of order 5% in the finite element solution for $a = 1.05$. Both $Q(p)$ and $Q'(p)$ elements are considered.

Table 9.1. CPU times for various combinations of ℓ and p to achieve approximately 5% accuracy for $a = 1.05$.

$Q(p)$				$Q'(p)$			
ℓ	p	Error %	time	ℓ	p	Error %	time
1	13	5.8	1.16	2	14	7.0	2.35
2	9	5.1	1.41	4	10	4.5	3.26
2	10	3.0	1.96	8	7	3.5	5.00
4	6	5.8	1.75	16	4	5.0	6.58
4	7	2.4	2.58				
8	4	5.8	2.58				
8	5	1.6	4.14				
16	3	3.2	5.73				

Table 9.2 shows the analogous timings required for accuracy of order 0.1%.

Table 9.2 CPU times for various combinations of ℓ and p to achieve approximately 0.1% accuracy for a = 1.05.

Q(p)				Q'(p)			
ℓ	p	Error %	time	ℓ	p	Error %	time
4	13	0.12	17.87	4	14	0.09	8.96
8	8	0.16	14.68	8	9	0.10	9.33
8	9	0.04	21.07	16	6	0.09	13.92
16	6	0.06	26.10				

We see that for a = 1.05 for both 5% accuracy and 0.1% accuracy the lowest cost occurs for smallest ℓ and large p. This is still more pronounced for a larger. For 5% accuracy the Q(p) element is less expensive than the Q'(p) element. In contrast the Q'(p) element was less expensive when 0.1% accuracy is required. This is consistent with the results of the analysis made in Section 4.

As discussed in [3] many factors contribute to the cost of the finite element solver, but cost tends to be dominated by the construction and condensation of the local stiffness matrices. For the data in Tables 9.1 and 9.2 there is one local matrix for each of ℓ^2 elements. For our particular model problems the local stiffness matrices for all elements are the same, so that considerable saving can be achieved by using one local matrix for all the elements. An estimate for the cost of implementing the solver this way is obtained from:

time using 1 local matrix

= total time - (time for ℓ^2 local matrix computations)

+ (time for local matrix computations)/ℓ^2

(Here in the local matrix computation both the construction and condensation is included.)

These timings, for 5% accuracy and 0.1% accuracy, are presented in Tables 9.3 and 9.4 respectively (for one processor computations). There is in general a dramatic drop in the total cost required by the finite element solver. The optimal combination is also tilted to high degrees. The comparison between the Q(p) and Q'(p) elements is consistent with the observations above. The Q(p) element is more efficient when low accuracy is obtained and Q'(p) is more efficient when high accuracy is required or the solution is smoother. The character of the optimal combination of ℓ and p seen here is in agreement with the results of an analysis of a computational model in [10].

Table 9.3. CPU times for various combinations of ℓ and p to achieve approximately 5% accuracy for a = 1.05 and one local stiffness matrix computation.

Q(p)				Q'(p)			
ℓ	p	Error %	time	ℓ	p	Error %	time
1	13	5.8	1.16	2	14	7.0	0.92
2	9	5.1	0.55	4	10	4.5	0.94
2	10	3.0	0.74	8	7	3.5	1.69
4	6	5.8	0.58	16	4	5.0	3.07
4	7	2.4	0.70				
8	4	5.8	1.02				
8	5	1.6	1.26				
16	3	3.2	2.61				

Table 9.4. CPU times for various combinations of l and p to achieve approximately 0.1% accuracy for a = 1.05 and one local stiffness matrix computation.

Q(p)				Q'(p)			
l	p	Error %	time	l	p	Error %	time
4	13	0.12	2.64	4	14	0.09	1.91
8	8	0.16	2.68	8	9	0.10	2.47
8	9	0.04	3.34	16	6	0.09	5.14
16	6	0.06	6.51				

Finally as observed in [3] the element oriented computations required by the solver used (with repeated stiffness matrix as in Table 9.1) allows a large amount of natural parallelism in the solution process. In Table 9.5 we show the CPU times and speedups for several choices of l and p on multiple processors of the Alliant FX/8 in comparison with computations reported in Table 9.1. We see typical speedups on eight processors between five and six.

Table 9.5 CPU times and speedups on multiple processors for various combinations of l and p that produce approximately 5% error for a = 1.05.

no. of processors	Q(p)				Q'(p)			
	l	p	time	speed up	l	p	time	speed up
8	4	7	0.51	5.06	4	10	0.59	5.53
8	8	5	0.76	5.45	8	7	0.87	5.45
8	16	3	1.15	4.98	16	4	1.24	5.31
4	2	10	0.62	3.17	2	14	0.71	3.31

Parallel efficiency is affected by such factors as the number of elements, the amount of work required per element and the storage requirements of the local

computations. For the data of Table 9.5, the largest speedup appear when $\ell = 8$. This is a consequence of the fact that there is considerable overhead for the relatively small number elements when $\ell = 4$ and for the small amount of work per element when $\ell = 16$. See [3] for a detailed study of such effects on parallel implementation.

The implementation we have used is not adaptive and hence the timing for the prescribed accuracy is not completely realistic because this accuracy is not known in advance. We can consider for example the p-adaptivity for given mesh where p is increased adaptively. Various aspects of such adaptive approaches will be discussed elsewhere.

References.

1. Ciarlet, P.G., [1978]: *The Finite Element Method for Elliptic Problems*, North-Holland, Amsterdam.

2. Babuška, I., Elman, H.C., [1989]: Some aspects of parallel implementation of the finite element method on message passing architectures, J. Comp. Appl. Math. **27**, 157-187.

3. Babuška, I., Elman, H.C., Markley, K., [1991]: Parallel implementation of the hp-version of the finite element method on shared memory architecture, to appear, SIAM J. Sci. Stat. Comp.

4. Babuška, I., Craig, A., Mandel, J., Pitharanta, J., [1991]: Efficient preconditioning for the p-version finite element method in two dimensions, SIAM J. Num. Anal. **28**, 624-661.

5. Szabo, B., Babuška, I., [1991]: *Finite Element Analysis*, John Wiley & Sons, New York, Chichester, Brisbane, Toronto, Singapore.

6. Walsh, J. L., [1960]: *Interpolation and approximation by rational functions in the complex domain*, third edition, American Math. Soc. Colloquium Publications, Vol. XX, American Math. Soc., Providence.

7. Berg, J., Löfström, J., [1976]: *Interpolation Spaces*, Springer-Verlag, Berlin, Heidelberg, New York.

8. Ahlfors, L.V., [1966]: *Complex Analysis*, McGraw-Hill, New York, St. Louis, San Francisco, Toronto, London, Sydney.

9. Betz, A., [1948]: *Konforme Abbildung*, (in German), Springer, Berlin, Göttingen, Heidelberg.

10. Babuška, I., Scapolla, T., [1987]: Computational aspects of the h, p and h-p versions of the finite element method, *Advanced in Computational Methods for Partial Differential Equations* VI, R. Vichnevetski, R.S. Stepleman (eds.), IMACS. Publ.

The Laboratory for Numerical Analysis is an integral part of the Institute for Physical Science and Technology of the University of Maryland, under the general administration of the Director, Institute for Physical Science and Technology. It has the following goals:

- To conduct research in the mathematical theory and computational implementation of numerical analysis and related topics, with emphasis on the numerical treatment of linear and nonlinear differential equations and problems in linear and nonlinear algebra.

- To help bridge gaps between computational directions in engineering, physics, etc., and those in the mathematical community.

- To provide a limited consulting service in all areas of numerical mathematics to the University as a whole, and also to government agencies and industries in the State of Maryland and the Washington Metropolitan area.

- To assist with the education of numerical analysts, especially at the postdoctoral level, in conjunction with the Interdisciplinary Applied Mathematics Program and the programs of the Mathematics and Computer Science Departments. This includes active collaboration with government agencies such as the National Institute of Standards and Technology.

- To be an international center of study and research for foreign students in numerical mathematics who are supported by foreign governments or exchange agencies (Fulbright, etc.).

Further information may be obtained from **Professor I. Babuška**, Chairman, Laboratory for Numerical Analysis, Institute for Physical Science and Technology, University of Maryland, College Park, Maryland 20742-2431.